

RESEARCH ARTICLE

10.1002/2016WR019839

Key Points:

- We apply a shape-free method to determine age distributions
- Our analysis was able to identify the occurrence of modern and current recharge periods
- The age of these events is consistent with knowledge of historically wetter periods

Correspondence to:

J. L. McCallum,
mcca0206@flinders.edu.au

Citation:

McCallum, J. L., P. G. Cook, S. Dogramaci, R. Purtschert, C. T. Simmons, and L. Burk (2017), Identifying modern and historic recharge events from tracer-derived groundwater age distributions, *Water Resour. Res.*, 53, 1039–1056, doi:10.1002/2016WR019839.


Received 23 SEP 2016

Accepted 6 JAN 2017

Accepted article online 13 JAN 2017

Published online 1 FEB 2017

Identifying modern and historic recharge events from tracer-derived groundwater age distributions

James L. McCallum^{1,2} , Peter. G. Cook^{1,2}, Shawan Dogramaci^{3,4}, Roland Purtschert⁵, Craig T. Simmons^{1,2}, and Lawrence Burk¹
¹School of the Environment, Flinders University, Adelaide, Australia, ²National Centre for Groundwater Research and Training, Flinders University, Adelaide, Australia, ³Rio Tinto Iron Ore, Perth, Australia, ⁴Ecosystems Research Group, School of Plant Biology, University of Western Australia, Crawley, Western Australia, Australia, ⁵Climate and Environmental Physics Division, Physics Institute, University of Bern, Bern, Switzerland

Abstract Understanding groundwater ages offers insight into the time scales of recharge, aquifer storage turnover times, and contaminant protection time frames. The ability to quantify groundwater age distributions heavily depends on the choice of the interpretive model, and often important features of the age distribution cannot be identified with the subset of available models. In this paper, we implemented a multiple tracer method using a technique that assumes limited details regarding the shape of the age distribution and applied it to dewatering wells at a mine site in the Pilbara region of north-western Australia. Using our method, we were able to identify distinct age components in the groundwater. We calculated the presence of four distinct age groups in the samples. All wells contained water aged between zero and 20 years. However, the rest of the samples were composed of water between 50 and 100 years, 100 and 600 years, or water approximately 1000 years old. These were consistent with local recharge sources (50–100 years) and knowledge of paleoclimate from lake sediment records. We found that although the age components were well constrained, the relative proportions of each component were highly sensitive to errors of environmental tracer data. Our results show that our method can identify distinct age groups in groundwater samples without prior knowledge of the age distribution. The presence of distinct recharge times gives insight into groundwater flow conditions over long periods of time.

1. Introduction

Many important questions in groundwater hydrology can be answered by determining the distribution of ages present in groundwater at one or multiple locations. These include aspects of groundwater recharge [McMahon *et al.*, 2011] and contaminant protection time frames for groundwater resources [Dörr *et al.*, 1995; Green *et al.*, 2010]. Groundwater age is best described as a distribution rather than a scalar property due to recharge and discharge patterns [Etcheverry and Perrochet, 2000; Cardenas, 2008], sampling conditions [Maloszewski and Zuber, 1982; Hofmann *et al.*, 2010], heterogeneity within the aquifer [Weissmann *et al.*, 2002; Engdahl *et al.*, 2012; McCallum *et al.*, 2014a], and transience [Engdahl *et al.*, 2016]. All these aspects are implicit to groundwater systems and so an understanding of groundwater age distributions is highly desirable.

One way of inferring groundwater ages is through the use of naturally occurring or ubiquitous anthropogenic compounds, collectively referred to as environmental tracers. Environmental tracers possess some form of concentration variation attributable to their recharge time. Variations may be due to changes in recharge concentration with time, or, some form of modification with increasing time since recharge (e.g., radioactive decay). Each of these variations corresponds to a specific time range. Information on the distribution of groundwater age is commonly obtained by measuring more than one tracer. A large number of tracers (e.g., ³H, ⁸⁵Kr, CFCs, SF₆) represent time frames less than 50 years. However, fewer tracers are available for larger time frames (e.g., ³⁶Cl, ⁴He, ¹⁴C, and ³⁹Ar).

Environmental tracers were originally used to determine specific ages of groundwater [Brinkman *et al.*, 1959]. This approach assumed that all water within a sample had the same age. Tracer-derived ages could then be used in conjunction with simple models to determine recharge [Vogel *et al.*, 1974] or flow rates within an aquifer [Bentley *et al.*, 1986]. Ideally it was assumed that tracer-derived ages approximated

advective ages. However, studies demonstrated that exchange with low conductivity zones [Sudicky and Frind, 1981; Sanford, 1997; Bethke and Johnson, 2002; Cornaton *et al.*, 2011] and dispersion [Ekwrzel *et al.*, 1994; Weissmann *et al.*, 2002] caused significant errors between tracer derived and theoretical ages. The use of a mean age or age mass that accounts for dispersive and diffusive processes has been proposed as an alternative to advective ages [Goode, 1996]. Environmental tracers have also been analyzed with models that describe the mixture of ages [Nir, 1964; Małoszewski and Zuber, 1982]. These models represent flow in specific geometries and under specific forcing [Leray *et al.*, 2016].

A specific drawback of tracer based studies is that some tracers may offer limited information about groundwater ages due to low temporal concentration gradients [Varni and Carrera, 1998; Waugh *et al.*, 2003; McCallum *et al.*, 2015], or multiple tracers may be correlated [Leray *et al.*, 2014], limiting useful interpretations of groundwater systems. The limitations of the use of individual tracers to infer groundwater ages were described by McCallum *et al.* [2015] and has also received attention recently as the concept of aggregation error [Kirchner, 2016; Stewart *et al.*, 2016]. Time series of environmental tracer data may also be useful [Stolp *et al.*, 2010; Massoudieh, 2013; McCallum *et al.*, 2014b], however, their collection requires continuous monitoring or the forethought of predecessors which is not always available in areas of current hydrological importance.

Another significant restriction of groundwater age studies is the limited subset of interpretive models of groundwater age used in conjunction with environmental tracer data. These models are based on simple assumptions of transport and sampling conditions [Małoszewski and Zuber, 1982]. However, over the past 35 years our understanding of how solutes move in groundwater systems has significantly improved, and the assumptions that underpin some of these models have been falsified. Given that both environmental tracers and groundwater age undergo similar transport, the assumption of one or multiple invalid models has a significant impact on the interpretations of groundwater systems made with such models. For example, assumptions of uniform recharge, perfect sampling conditions, and the distribution of flow through the entire depth of the aquifer can impact the results of model interpretations. Recent studies have investigated the use of nonparametric or shape-free methods for estimating groundwater ages [Massoudieh *et al.*, 2014; Visser *et al.*, 2013; McCallum *et al.*, 2014b]. These techniques are based on advances in other areas including stream tracer testing, bank infiltration, and aquifer tracer testing [Fienen *et al.*, 2006; Cirpka *et al.*, 2007; Payn *et al.*, 2008 and others]. The benefit of these techniques is not fixed; only constraints refer to nonnegativity and potentially the smoothness of the distribution. The disadvantage, however, is that the methods require a long-time series of concentration observations, which may not be available when sampling at a single time. Alternatively, the number of discrete ranges of age bins may be reduced which prevents detailed information about the age distribution from being identified.

A further significant challenge in groundwater studies lies in assessing the impact of large changes in the hydrological system on groundwater resources. The most basic definition of groundwater age is the time since water was recharged. Transience may be observed using a time series of environmental tracer data [Manning *et al.*, 2012; Massoudieh, 2013] and may also be evident as distinct recharge events [Schwartz *et al.*, 2010]. A possible hypothesis is that groundwater ages may represent a combination of recharge events or wet periods, rather than a quasicontinuous mixture of ages. These individual events may be due to seasonality [Jasechko *et al.*, 2014], intensive rainfall events [Taylor *et al.*, 2012a; Jasechko *et al.*, 2015], or climate variability [Taylor *et al.*, 2012b].

In this paper, we apply a multitracer technique using ^3H , ^{85}Kr , CFCs, SF_6 , ^{39}Ar , and ^{14}C to assess the groundwater age distribution at a site where mine dewatering for iron-ore production has led to large changes in the groundwater system over a short period of time. We implement a nonparametric technique to identify age distributions without the assumption of a distribution a priori, and attempt to identify if large changes in the groundwater flow system are evident in the groundwater age distribution obtained at a single time. The approach here differs from previous methods as it uses a comprehensive set of environmental tracers to inform detailed groundwater age distributions.

2. Site Description

The study was undertaken in the vicinity of the Hope Downs 1 iron ore mine in the Hamersley Basin in the Pilbara region of north-western Australia (Figure 1). Iron ore production at the site is from the Marra Mamba

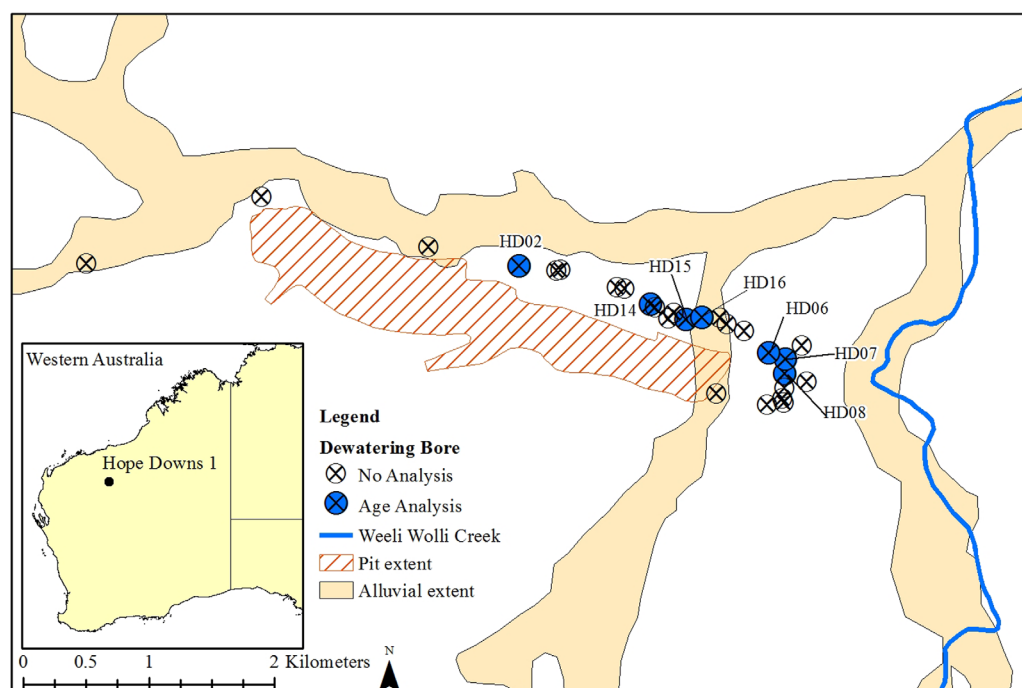


Figure 1. Field site location and the location of dewatering bore, alluvium, the dewatered pit, and Weeli Wolli Creek.

Iron Formation. The Marra Mamba formation is overlain by the Wittenoom formation which is composed of dolomites and shales and is considered to be a major aquifer in the area (Figure 2). The site lies within the Weeli Wolli Creek Catchment, where the main channel and tributaries flow after high intensity rainfall events, mostly occurring between the months of December and March [Dogramaci *et al.*, 2012]. Shallow alluvial deposits occur adjacent to the main streams and tributaries. The site is bounded to the East and North by shallow alluvial systems, and another alluvial system bisected the pit prior to excavation (Figure 2).

Groundwater in the greater Hamersley basin has been identified as having an isotope signature similar to rainfall events of 20 mm or more, suggesting that recharge occurs during high intensity events [Dogramaci *et al.*, 2012]. On a longer time scale, a number of wet and dry periods have been identified from sediment records by Rouillard *et al.* [2016]. The authors found that the period between 1990 and present has been the wettest of the last 2000 years. The 400 years prior to 1990 was generally dry with a number of sporadic megafloods, and the 800 years prior (400–1200 years before present) had more consistent stream flows,

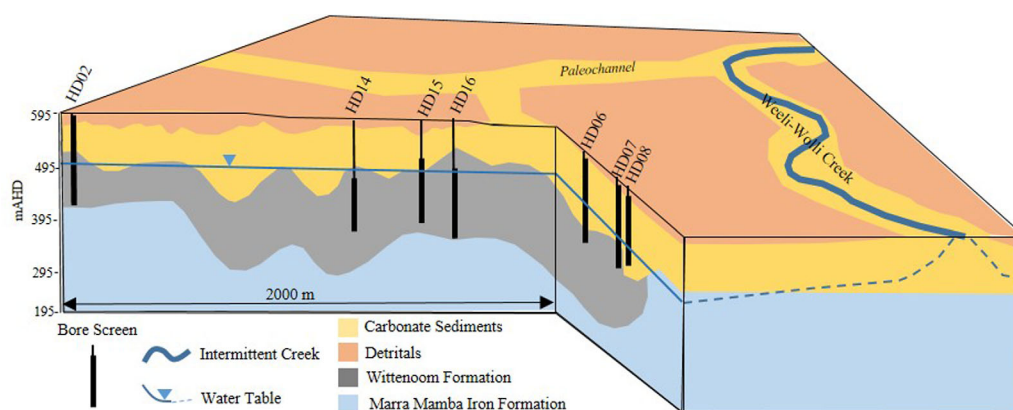


Figure 2. 3-D cross section of bore locations, premining water tables, and the geology of the field site. Modified from Cook *et al.* [2016].

suggesting a wetter climate. The authors also found that the period between 1200 and 1900 years before present was the most arid of the past 2000 years.

Dewatering in the area to support iron ore production commenced in 2007. To achieve dry mining conditions up to 80 ML/d of mine surplus water is discharge into Weeli Wolli creek 10 km down gradient of the study area. The premining groundwater flow was from west to east with the water discharging to the alluvial system surrounding Weeli Wolli Creek (Figure 1). Discharge to the alluvium is driven by evapotranspiration. In addition to the regional discharge, the alluvium also receives recharge from floods. Since 2007, groundwater drawdowns of up to 80 m have been observed in the vicinity of the pit, with drawdowns greater than 10 m observed for an area of 8 km² [Cook *et al.*, 2016].

3. Method

3.1. Tracer Data

Water samples were collected in August 2014 and August–September 2015 from outlets connected to the mine dewatering bores. Samples collected in 2014 were analyzed for CFCs (CFC-11, CFC-12, and CFC-113), SF₆, ³H, and ¹⁴C. The sampling and analytical techniques for these samples are detailed in Cook *et al.* [2016] and is only briefly repeated here. Carbon-14 and ¹³C were collected in 1 L plastic bottles and analyzed by AMS and IRMS, respectively at the GNS Rafter Radiocarbon Laboratory. Samples for CFC-11, CFC-12, and CFC-113 were collected in 125 mL glass bottles. The sample bottles were filled and flushed while submerged in a bucket of water. CFC concentrations were determined by gas chromatography at the GNS Water Dating Laboratory.

Tritium samples were also collected in 1 L plastic bottles and analyzed using the method of *Morgenstern and Taylor* [2009] also at the GNS Water Dating Laboratory. SF₆ samples were collected in submerged 1 L bottles and analyzed at the GNS Water Dating Laboratory using gas chromatography.

In addition to previously collected data, ³⁹Ar, ³⁷Ar, and ⁸⁵Kr concentrations were obtained in 2015 from gas samples taken in situ. Between 3.3 and 4.3 cubic metres of water were degassed in the field to obtain gas samples of 6.5 Bar in six kilogram cylinders [Purtschert *et al.*, 2013]. The samples were analyzed using low level gas proportional counting at the University of Bern, Switzerland [Loosli *et al.*, 1986; Loosli and Purtschert, 2005; Riedmann and Purtschert, 2016].

3.2. Atmospheric Signals

The use of environmental tracers in age studies relies on the accurate quantification of recharge concentrations. Tracers including CFCs, SF₆, ⁸⁵Kr, ¹⁴C, and ³⁹Ar have relatively consistent atmospheric concentrations. In this study, we have adopted southern hemisphere concentrations for CFCs and SF₆ as reported by Bullister [2015]. Carbon-14 concentrations were extrapolated from data presented by Manning *et al.* [1990]. The atmospheric input for ³⁹Ar is constant globally at 100% modern [Corcho Alvarado *et al.*, 2007].

Radioactive tracers with short half-lives are more variable in the atmosphere. Appropriate input concentrations rely on the proximity of a site to bomb testing or nuclear facilities. Bomb testing in Australia was carried out in the Monte Bello Islands (located 130 km from the Pilbara region) between 1952 and 1957 [Tadros *et al.*, 2014]. As no time series was available directly at the field site, extrapolation of bomb peak data was undertaken using data from Perth, Adelaide, Darwin, and Alice Springs [IAEA/WMO, 2016]. A single measurement of rainwater at the site was collected in 2015 having a concentration of 1.5 TU which was assumed to be representative of pre and postbomb peak concentrations and is in good agreement with the spatial interpretation presented by Tadros *et al.* [2014]. Tritium may also be produced in trace amounts in the subsurface [Lehmann *et al.*, 1993]; however, we have assumed this to be negligible.

Krypton-85 may also be variable in the atmosphere [Winger *et al.*, 2005; Corcho Alvarado *et al.*, 2007; Althaus *et al.*, 2009]. The shape of the continuous curve used was obtained from data presented in Bollhöfer *et al.* [2014], Ross [2010], and Weiss *et al.* [1992]. Although these measurements were not taken directly at the site, Bollhöfer *et al.* [2014] demonstrated that the concentration of atmospheric ⁸⁵Kr was well mixed in the southern hemisphere. The recharge concentrations used in this study are presented in Figure 3.

In addition to variations in the atmospheric signal, tracer concentrations are also modified by radioactive decay with known decay rate coefficients for radioisotopes. Degradation of CFCs may also be represented

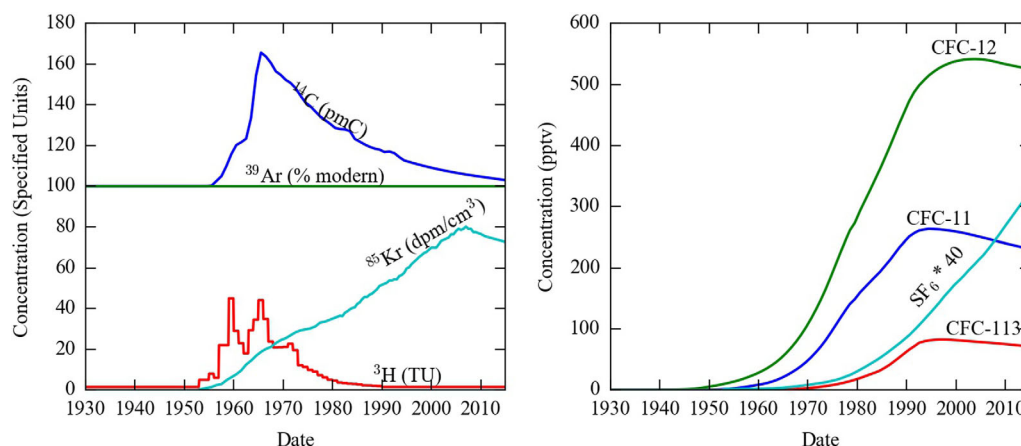


Figure 3. Atmospheric/recharge concentrations adopted for the study. The units for ^{14}C , ^{39}Ar , ^{85}Kr , and ^3H are specified on the figure. The scale for SF_6 is also specified on the figure.

similarly to decay [Hinsby et al., 2007; Massoudieh et al., 2012]. As the rate coefficients of CFC degradation are unknown, we included the estimation of these coefficients in our analysis. The decay constants are presented in Table 1.

3.3. Deconvolution

The relationship between observed groundwater concentrations (c_g), recharge concentrations at the water table (c_r), and the groundwater age distribution of saturated groundwater (g) can be given as:

$$c_g = \int_0^{\infty} c_r(t-\tau) \cdot g(\tau) \cdot \exp(-\lambda\tau) \cdot d\tau \quad (1)$$

where t is time, τ is the variable of integration, and λ is the radioactive decay constant. For tracers not experiencing radioactive decay, the exponential term reduces to one. One of the key differences between gas tracers and water movement is travel through the unsaturated zone which is important as tritium moves considerably differently than gas tracers [Cook and Solomon, 1995]. The concentration of tritium will represent a combined travel time through the unsaturated zone and the saturated zone. The total travel time distribution is the convolution of the two individual travel time distributions [e.g., Sardin et al., 1991]:

$$g_t = g_u * g \quad (2)$$

where g_u is the residence time distribution through the unsaturated zone, g_t is the total residence time distribution through the unsaturated and saturated zones, and the symbol $*$ represents the convolution integral. Here we will make the assumption of a piston flow time lag (τ_L) through the unsaturated zone such that $g_t = \delta(\tau_L) * g$. A modified form of equation (1) can be written to account for a corrected tritium concentration at the water table:

$$c_g = \int_0^{\infty} c_r(t-\tau-\tau_L) \cdot g(\tau) \cdot \exp(-\lambda[\tau+\tau_L]) \cdot d\tau \quad (3)$$

Table 1. Decay Constants for Modeled Tracers	
Tracer	Decay Constant (yr^{-1})
^{14}C	1.21×10^{-4}
^{39}Ar	2.58×10^{-3}
CFC-11	Unknown
CFC-12	Unknown
CFC-113	Unknown
SF_6	0
^3H	5.65×10^{-2}
^{85}Kr	6.44×10^{-2}

hence this corrected form of the equation can be used to account for the decay of tritium in the unsaturated zone prior to reaching the water table. It is assumed that the gas tracers show no lag time.

In most studies, the form of g is predetermined from a single or a subset of models [Massoudieh et al., 2012]. Many of these models assume specific sampling conditions, simple transport mechanisms, or one-dimensional flow. In this study, our intention is to determine the shape of g based on concentration observations and the constraint of smoothness, which is achieved by writing the

equations in discrete form for nc groundwater tracer concentrations and ng discrete values of g as [Cirpka et al., 2007]:

$$\mathbf{c}_g = \mathbf{X}\mathbf{g} \quad (4)$$

where \mathbf{c}_g is an $nc \times 1$ vector of measured concentrations, \mathbf{X} is an $nc \times ng$ matrix of historic recharge data, and \mathbf{g} is an $ng \times 1$ vector of discrete values of the age distribution. If the concentrations are from many different tracers sampled at a single time (t), and the step between discrete values of age is constant, then the discrete values of \mathbf{X} can be given as:

$$\mathbf{X}_{ij} = \mathbf{c}_{ri}(t - \tau_j) \cdot \exp(\lambda_i \tau_j) \cdot d\tau_j \quad (5)$$

where τ_j is the j th discrete value of age, and c_{ri} and λ_i are specific to the i th tracer. In cases where the difference between discrete values of age varies, and becomes large, the central age value for any interval is not representative for nonlinear variations. This is because the mean concentration is not equivalent to the concentration of the mean age [Park et al., 2002]. Therefore, the following definition should be used:

$$\mathbf{X}_{ij} = \int_{\tau_j - d\tau_j/2}^{\tau_j + d\tau_j/2} \mathbf{c}_{ri}(t - \omega) \cdot \exp(\lambda_i \omega) \cdot d\omega \quad (6)$$

where ω is the variable of integration. In this expression the assumed probability density of ages within a discrete bin with duration $d\tau$ is constant. For radioactively decaying tracers with constant input, equation (6) can be evaluated analytically. For tracers with a variable atmospheric input, equation (6) requires numerical integration. Equation (6) can also be modified to account for the unsaturated zone lag of tritium.

A number of additional constraints including nonnegativity, smoothness, and integration are also needed. These have been explained previously and are included in Appendix A. The procedure here requires the observed concentrations, specified errors, and a choice of the discretization of age. The procedure outlined in the appendix determines the weighting of the smoothness constraint and returns the best nonnegative estimate of the age distribution and error bounds. In the rest of this section, we will outline the choices of observation errors and discrete values of age.

The age distribution was discretized by 1 year intervals between zero and 60 years, 10 year intervals between 60 and 200 years, 25 year intervals between 200 and 1100 years, 50 year intervals between 1100 and 2000 years, and 100 year intervals between 2000 and 20,000 years. Thus smaller intervals were chosen to represent the ages where multiple tracers were present in recharge, and larger intervals were used when limited data were available. The upper bound of 20,000 years was selected as this is the point where contributions of ^{14}C generally become negligible due to decay. By truncating the age distribution, we assume that no water is present at ages larger than the limit.

The errors applied to the individual concentrations were selected to be consistent with reported analytical error with the exception of ^{14}C . Carbon-14 concentrations required the use of a corrective model open system carbonate dissolution [Han and Plummer, 2013]. This model also requires concentrations of $\delta^{13}\text{C}$ and HCO_3^- , in addition to measurements of pH and temperature. Each of these measurements also contained errors. The assumption of the corrective model also introduces further errors. The error of ^{14}C was set to be 20% of the measurement to account for these errors. No additional errors were added to other tracers to account for structural errors, as unknown structural components of CFC degradation and unsaturated zone time lags were estimated as part of the analysis.

3.4. Estimation of Tritium-Unsaturated Zone Time Lags and CFC Degradation

The analysis described above assumes that all components of the linear system are known a priori which is not the case for estimating the unsaturated zone time lags and the degradation of CFCs. Parameters relating to degradation and unsaturated zone time lags were estimated using the simplex method of Nelder and Mead [1965] in conjunction with the deconvolution procedure. The approach implemented the following steps:

1. Start with an initial estimate of parameters,
2. Perform deconvolution to obtain an initial estimate of g and record the initial objective function and parameters,

Table 2. Parameters for Estimation of Unknown Components of Linear Equations

Parameter	Units	Initial Estimate	Initial Interval
CFC-11 degradation	yr ⁻¹	0.347	0.04
CFC-12 degradation	yr ⁻¹	0.047	0.04
CFC-113 degradation	yr ⁻¹	0.131	0.04
Tritium unsaturated zone lag	years	15.0	0.25

3. Use the Nelder-Mead method with the current estimate of g to predict new parameters,
4. Perform deconvolution to obtain a new estimate of g and record the current objective function and parameters,
5. Repeat steps 3 and 4 for a determined number of times, and
6. Return the parameters that result in the best objective function.

The objective function was computed as:

$$\phi = \sum_{i=1}^{nt} \frac{1}{\sigma_i^2} (c_{obs,i} - c_{est,i})^2 \quad (7)$$

where nt is the number of tracers, σ_i is the error of the i th tracer, and c_{obs} and c_{est} are the observed and estimated concentrations, respectively. The objective function used all tracer concentrations, not just those with unknown parameters.

Initial estimates were obtained by using the procedure above to fit the concentration data from all of the wells simultaneously. Table 2 presents the initial estimates and initial intervals for the Nelder-Mead simplex method. For each individual well, the objective functions were calculated for 10 iterations of the Nelder-Mead simplex method. Generally, the best parameters were found in less than three iterations.

3.5. Determination of Error Bounds

Error bounds of estimated methods were found by boot strapping that is, perturbing the measured data using a simple Monte-Carlo method. The measured points were assumed to have a mean of the measured value and a standard deviation of the measurement error. The distributions were reflected about zero to prevent negative values. The distributions of each of the measurements were sampled independently 1000 times. For each realization, the deconvolution procedure and estimate of unknown parameters were undertaken. For the realizations using the perturbed data, the Nelder-Mead simplex approach used the value obtained from the unaltered estimates as an initial guess.

3.6. Age Distribution Metrics

In addition to the complete age distribution, metrics of it may also be used. A metric of particular interest is the fraction of young water which is often used as it is identifiable due to the large number of tracers present in recharge water since the 1950s. Water of this age represents a valuable yet finite resource [Gleeson *et al.*, 2016]. Here we define young water as water with an age smaller than 60 years. The young fraction of the age distribution is simply the value of the cumulative age distribution at 60 years. This young fraction has been used extensively in groundwater studies [Solomon *et al.*, 2010; Massoudieh *et al.*, 2012; McCallum *et al.*, 2014b; Gleeson *et al.*, 2016; Jasechko, 2016; and others].

The mean age is also of interest and can be obtained by:

$$A_\mu = \int_0^\infty g(\tau) \tau \cdot d\tau \quad (8)$$

where A_μ is the mean age. The mean age can be compared directly to modelled values simulated using the equations of Goode [1996]. The mean groundwater age may be underestimated because we truncated the age distribution at 20,000 years, whereas the young fraction is unaffected by the truncation.

4. Results

4.1. Tracer Data

The measured environmental tracer concentrations are presented in Table 3. Carbon-14 concentrations varied between 31.84 and 44.94 pmC. Uncorrected, these samples represent piston flow ages of between 6600 and 9500 years. However, significant variation in the $\delta^{13}\text{C}$ is also observed. To account for the variation of

Table 3. Analytical Results for Groundwater Samples

Well	^{14}C (pmC)		$\delta^{13}\text{C}$ (‰)		HCO_3^- (mg/L)		pH (pH units)		T (°C)		^{39}Ar (% modern)	
HD16	34.85	±0.1	−11.12	±0.2	400	±10	7.9	±0.1	30.26	±0.1	55	±11
HD15	33.98	±0.1	−10.94	±0.2	410	±10	7.9	±0.1	30.04	±0.1	31	±6.2
HD14	31.84	±0.1	−10.79	±0.2	470	±10	7.8	±0.1	30.22	0.1	56	±11.2
HD02	31.86	±0.1	−10.23	±0.2	460	±10	7.9	±0.1	30.76	0.1	31	±6.2
HD08	44.94	±0.1	−11.33	±0.2	470	±10	7.9	±0.1	27.3	0.1	83	±16.6
HD07	44.38	±0.1	−11.7	±0.2	400	±10	8	±0.1	27	0.1	100	±20
HD06	41.42	±0.1	−11.36	±0.2	460	±10	7.9	±0.1	28.09	0.1	69	±13.8
Well	CFC-11 (pptv)		CFC-12 (pptv)		CFC-113 (pptv)		SF_6 (pptv)		Tritium (TU)		^{85}Kr (dpm/cm ³)	
HD16	5.3	±1	61.8	±8.4	0.7	±3.6	0.1	±0.05	0.049	±0.016	11.9	±0.8
HD15	3.4	±1.4	45.8	±10.7	0	±7.7	0.09	±0.08	0.086	±0.016	16.2	±1.4
HD14	1	±1	13.6	±6.2	0	±7.7	0.17	±0.1	0.003	±0.016	6.7	±1.34
HD02	16.4	±2.6	109	±15.6	8.8	±7	0.04	±0.04	0	±0.016	7.8	±1.1
HD08	18.4	±3	85	±12	5.4	±9.2	0	±0.08	0.085	±0.016	9.1	±1
HD07	16.9	±2.1	90.7	±11.3	6.2	±7.2	0.07	±0.06	0.098	±0.016	19.3	±0.8
HD06	10.3	±1.6	67.4	±9.3	1.5	±7.3	0.07	±0.07	0.026	±0.016	12.2	±1.2

$\delta^{13}\text{C}$, the initial ^{14}C activity, presented in Figure 2 was corrected using the Mook model [Han and Plummer, 2013]. The model assumed an initial $\delta^{13}\text{C}$ value of -21.00 and a carbonate activity from the Wittenoom Formation dolomite of 0 pmC [Becker and Clayton, 1972]. The other parameters required for the Mook model are presented in Table 3.

Argon-39 concentrations ranged between 31 and 100% modern. These concentrations correspond to piston flow ages between 0 and 455 years. Argon-39 is possibly produced within the matrix. Three samples, HD16, HD14, and HD06 were also analyzed for ^{37}Ar . Argon-37 and ^{39}Ar are both neutron activation products, however ^{37}Ar has a half-life of 35 days hence elevated ^{37}Ar concentrations indicate subsurface production [Corcho Alvarado et al., 2013; Edmunds et al., 2014]. Each of the three samples reported concentrations below detection limit, making subsurface production of ^{39}Ar unlikely so that the high ^{39}Ar concentrations most likely indicate young water contributions.

CFCs and SF_6 were corrected for excess air and related back to atmospheric concentrations, as described by Busenberg and Plummer [2000, 2008]. Equivalent atmospheric CFC-11 concentrations ranged between 1 and 18.4 pptv. CFC-12 concentrations ranged between 13.6 and 109 pptv. There is some disparity between CFC-11 and CFC-12. For example, groundwater sampled from HD02 had CFC-12 concentrations which were 20% of present atmospheric concentrations, whereas CFC-11 concentrations were only 7% of present concentrations. CFCs may also experience varying levels of degradation [Hinsby et al., 2007], and CFC-11 typically shows stronger degradation than CFC-12. CFC113 concentrations ranged between 0 and 8.8 pptv and SF_6 concentrations ranged between 0 and 0.17 pptv. The SF_6 concentrations were much lower than expected compared to CFCs. The likely reason for the low concentrations is degassing [Visser et al., 2009]. SF_6 was excluded from further age analysis due to the observed degassing.

Tritium concentrations varied between 0 and 0.098 TU. Tritium is part of the water molecule itself. All other tracers are dissolved gasses which can lead to some differences between the travel time indications due to variable saturated conditions between the land surface and the water table [Cook et al., 1995]. If we assume that water was recharged with a present day concentration of 1.5 TU, these concentrations represent piston flow ages of 48 years and greater. Krypton-85 concentrations varied between 6.7 and 12.9 dpm/cm³. The modern atmospheric concentration of ^{85}Kr is 75 dpm/cm³ indicating a large portion of young water in the samples. The error bounds of ^{85}Kr are relatively high due to a low recovery of total Kr which is consistent with the observation of SF_6 degassing. However, because the value for ^{85}Kr (and ^{39}Ar) is based on the isotope ratio $^{85}\text{Kr}/\text{Kr}$ (or $^{39}\text{Ar}/\text{Ar}$), the dating relationships are unaffected by degassing.

4.2. Groundwater Ages

Figure 4 presents a comparison of the measured concentrations and concentrations estimated with the deconvolution procedure. All tracers follow a general 1:1 line indicating a good fit. For most tracers, the predicted ranges are much lower than the range of estimated errors due to the tracers being modified independently. The simultaneous fitting of multiple tracers likely inhibits the prediction of the most extreme values.

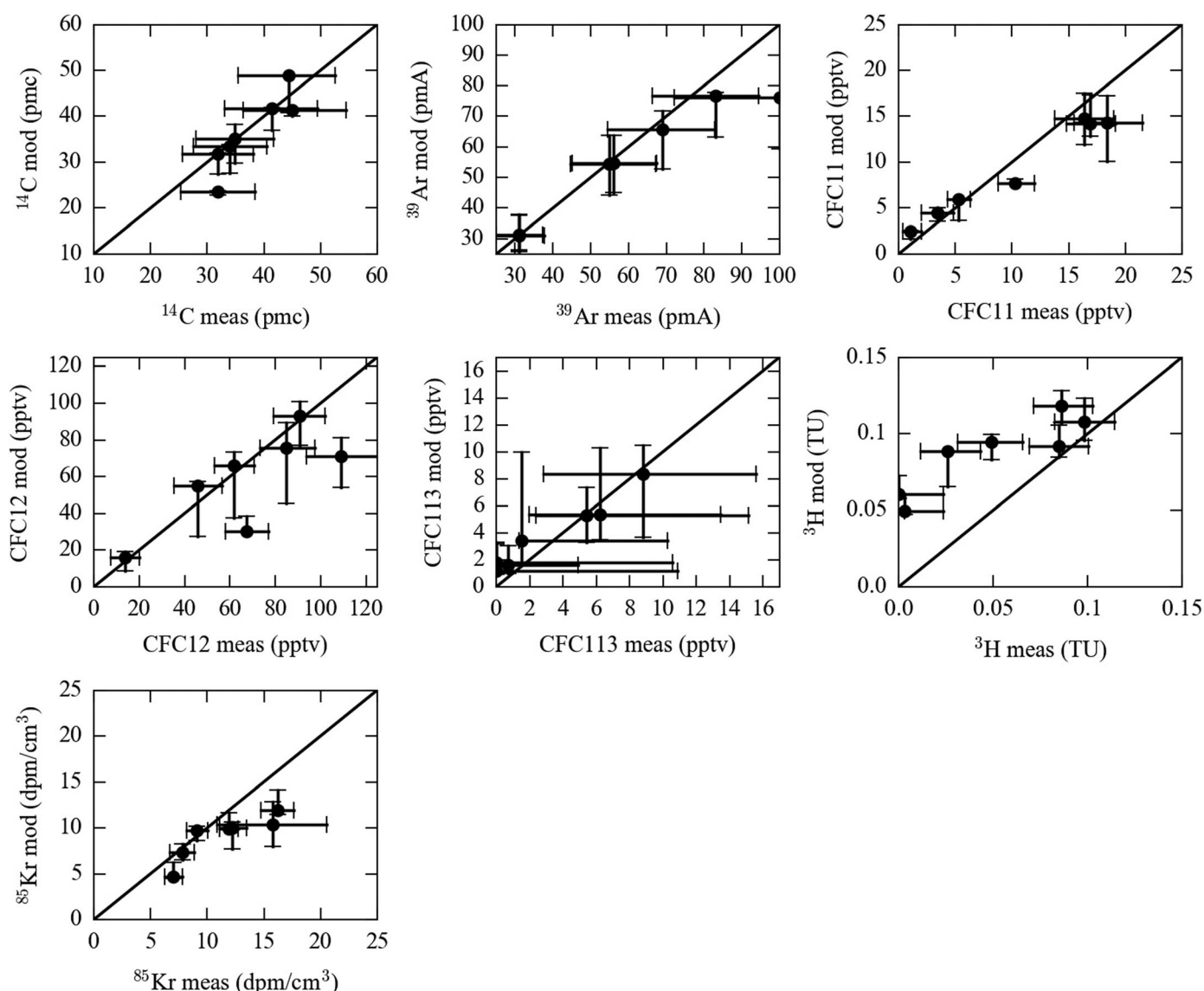


Figure 4. Plots of measured and modeled concentration. Error bars represent the central 68% of the cumulative distributions obtained through the concentration perturbation.

The predicted age distributions are presented in Figure 5. All wells contain a fraction of water less than 20 years old indicative of recently recharged water which may be due to the intersection of the water table by the screens pumping wells. By accounting for the lag of tritium and assuming rapid transport of gas tracers, the water table effectively represents a zero age boundary. Gas tracers will also experience a lag in the unsaturated zone; however, gas tracers are considered to move much faster than water movement [Cook and Solomon, 1995; Schwientek et al., 2009]. The proportion of young water is discussed in greater detail in a subsequent section.

A second component with ages between 50 and 200 years is observed in wells HD07 and HD08. These wells occur in close proximity to each other and also close to the alluvial system around Weeli-Wolli Creek. This range of ages may how long water takes to travel from the Creek, when being recharged during floods, to the observation wells.

A third age component of between 100 and 600 years is observed in wells HD06, HD14, and HD16. All of these wells are screened predominantly in the Wittenoom formation (Figure 2). This range of ages may be indicative of the travel time of recharged water to the location of the wells within this formation.

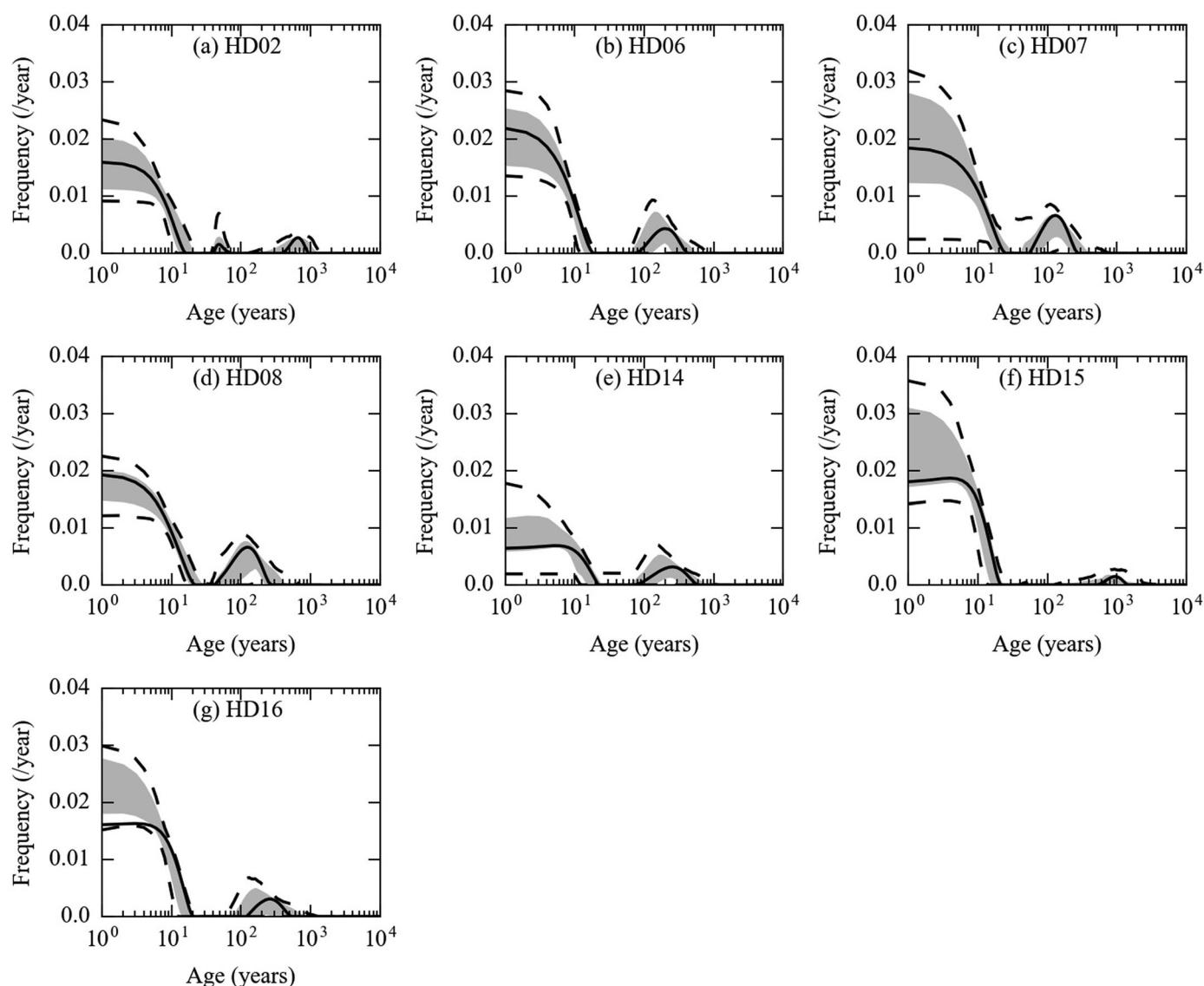


Figure 5. Predicted groundwater age distributions. Solid black lines represent the estimates made with the unaltered data. Grey-shaded areas represent the central 68% of estimated values using the perturbed data. The dashed black lines represent 95% of the cumulative distributions of the perturbed data. The locations of the wells are presented in Figures 1 and 2.

A fourth age component of approximately 1000 years is present at the location of boreholes HD02 and HD15. Interestingly, these boreholes are also both screened in the Wittenoom formation; however, the older age component is quite different. HD02 also contains a component of water approximately 30 years old.

The range of errors of the estimates are also of interest. The figures suggest that while the relative proportions of different ages are difficult to constrain, the range of ages present in the samples seem to occur in the same place. This consistency suggests that while it may be difficult to determine an exact distribution of ages, the main components are still identifiable from the multitracer approach.

4.3. Degradation and Lag Time Estimates

Table 4 represents the best estimates of the degradation and unsaturated zone lag for each of the wells. Although some variation exists between wells the degradation represents the expected trend that CFC-11 degrades more quickly than CFC-12 [Hinsby *et al.*, 2007]. Interestingly, the degradation coefficients show groupings also. Wells screened to the North of the pit—HD06, HD14, HD15, and HD16 have similar degradation characteristics, whereas the two wells closest to Weeli-Wolli Creek HD07 and HD08 have different but also consistent degradation rate coefficients which may be indicative of the water sources or the

Table 4. Best Estimates of Unknown Parameters and Metrics^a

Parameter	Units	HD02	HD06	HD07	HD08	HD14	HD15	HD16
CFC-11 degradation	yr ⁻¹	0.187	0.63	0.27	0.27	0.63	0.94	0.63
CFC-12 degradation	yr ⁻¹	0.00	0.33	0.03	0.05	0.20	0.15	0.07
CFC-113 degradation	yr ⁻¹	0.03	0.41	0.21	0.21	0.41	0.73	0.73
Tritium-unsaturated zone lag	Years	19.8	16.8	15.8	17.8	14.8	15.5	17.0
Metric								
Mean age	Years	550	177	110	108	254	716	2090
Young fraction		0.15	0.18	0.21	0.21	0.10	0.24	0.20

^aThe location of the wells is presented in Figures 1 and 2.

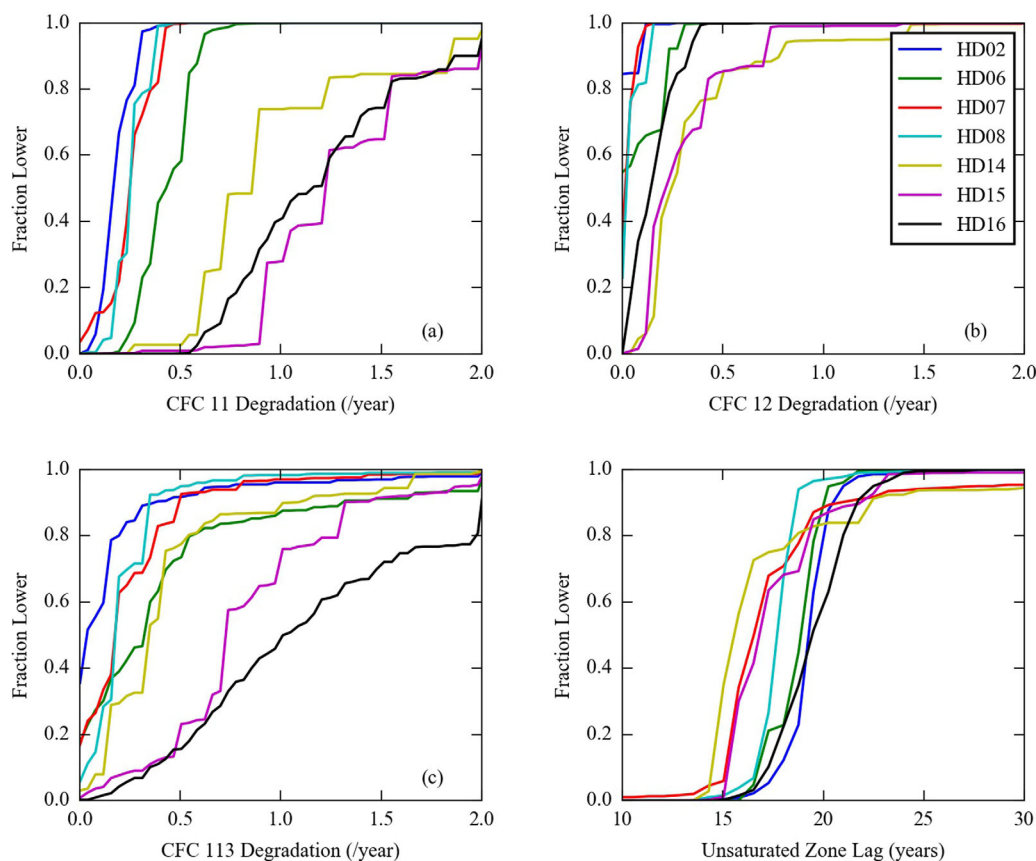
geochemical and microbial processes occurring in the different aquifers. As mentioned above, these two groups are predominantly screened in different aquifer materials.

The ranges of values predicted for degradation rate coefficients are presented in Figure 6. Generally, locations where a lower degradation rate coefficient was predicted have more constrained values. The groupings of wells are also apparent in the distribution of parameters. For example, the CFC-11 degradation at sites HD14, HD15, and HD16 are very similar.

The best estimates of lag times ranged between 14.8 and 19.8 years (Table 4). Tritium has a half-life of 12.3 years suggesting that travel in the unsaturated zone more than halves the rainfall concentration. The predicted range of unsaturated zone lags for all wells generally lie between 15 and 25 years.

4.4. Mean Age and Young Fraction

The best prediction of the mean ages is presented in Table 4. Mean ages range between 108 and 2090 years. The two wells close to Weeli-Wolli Creek (HD07 and HD08) report similar mean ages. However, the


Figure 6. Cumulative distributions of estimates of unknown parameters using perturbed data. Location of wells is shown in Figures 1 and 2.

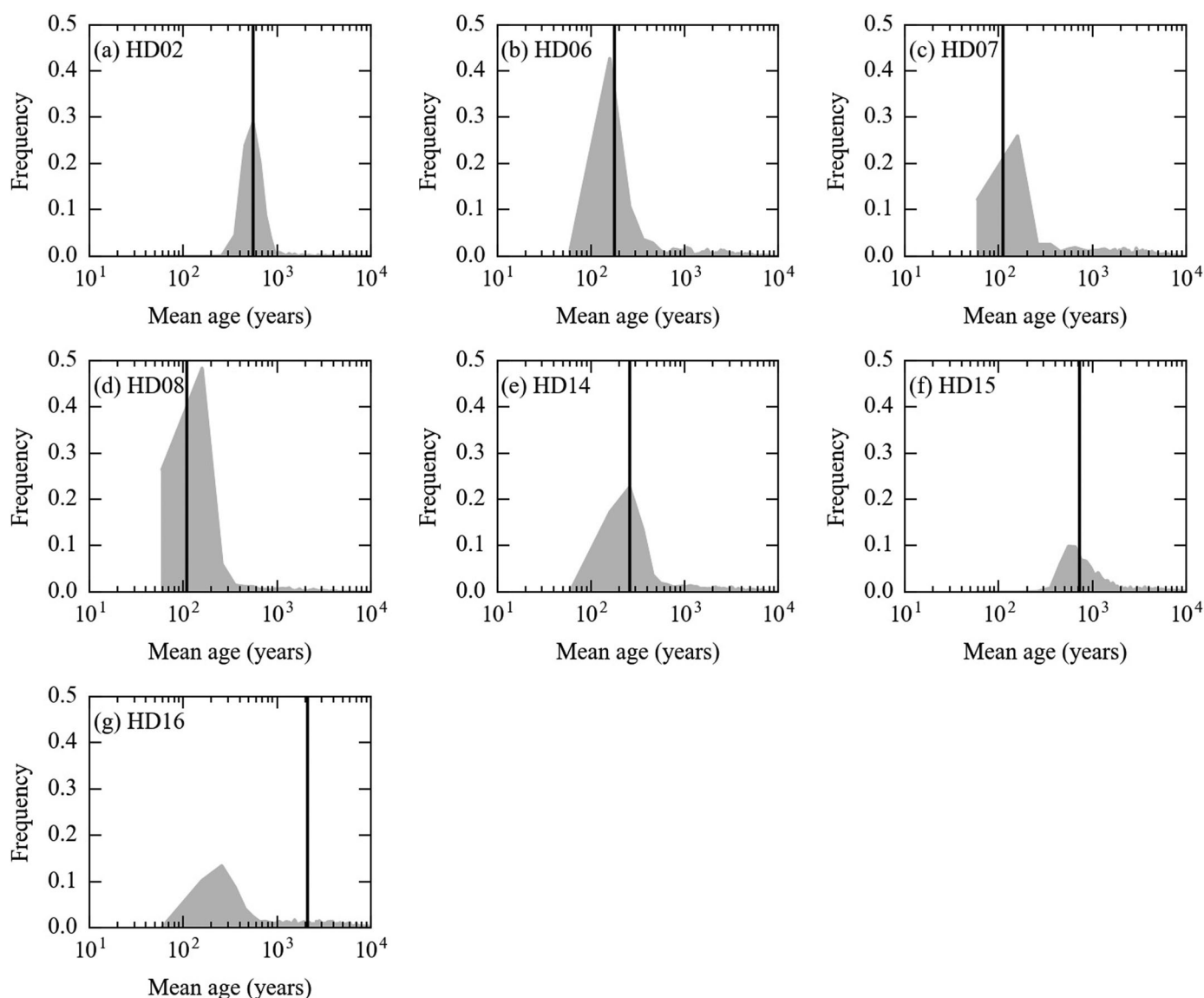


Figure 7. Distributions of estimates of mean ages from perturbed data. Solid black line represents best estimate (Table 4). The location of the wells is presented in Figures 1 and 2.

other wells have inconsistent mean ages. Figure 7 presents the distributions of mean age predictions for each of the wells. The predicted range of mean ages is quite large. As described above, the method implemented suggests that the ages present in a sample can be identified, however, the proportion of these components are difficult to constrain. The mean age is sensitive to the variations of the proportion of the older component leading to a large range in the ages.

By normalizing the age distribution to one, we specify that the whole distribution has to be defined within the given ranges. Tracer data for six of the seven wells are able to be explained by water components within the specified age range only. However, for groundwater collected from well HD16, this constraint forced some water to be included in the oldest bin. This is evident in the high mean age of the best estimate and the distribution of mean age estimates (Table 4, Figure 7g). The fact that the water cannot be explained by the ranges covered by the tracers used here also leads to an error.

The range of the young fraction appears more constrained than mean ages (Figure 8). The young fraction is indicative of recent recharge. Many of the tracers used show some variation over the past 60 years (Figure 3), increasing the amount of data available to constrain this time frame. Although the fraction of young

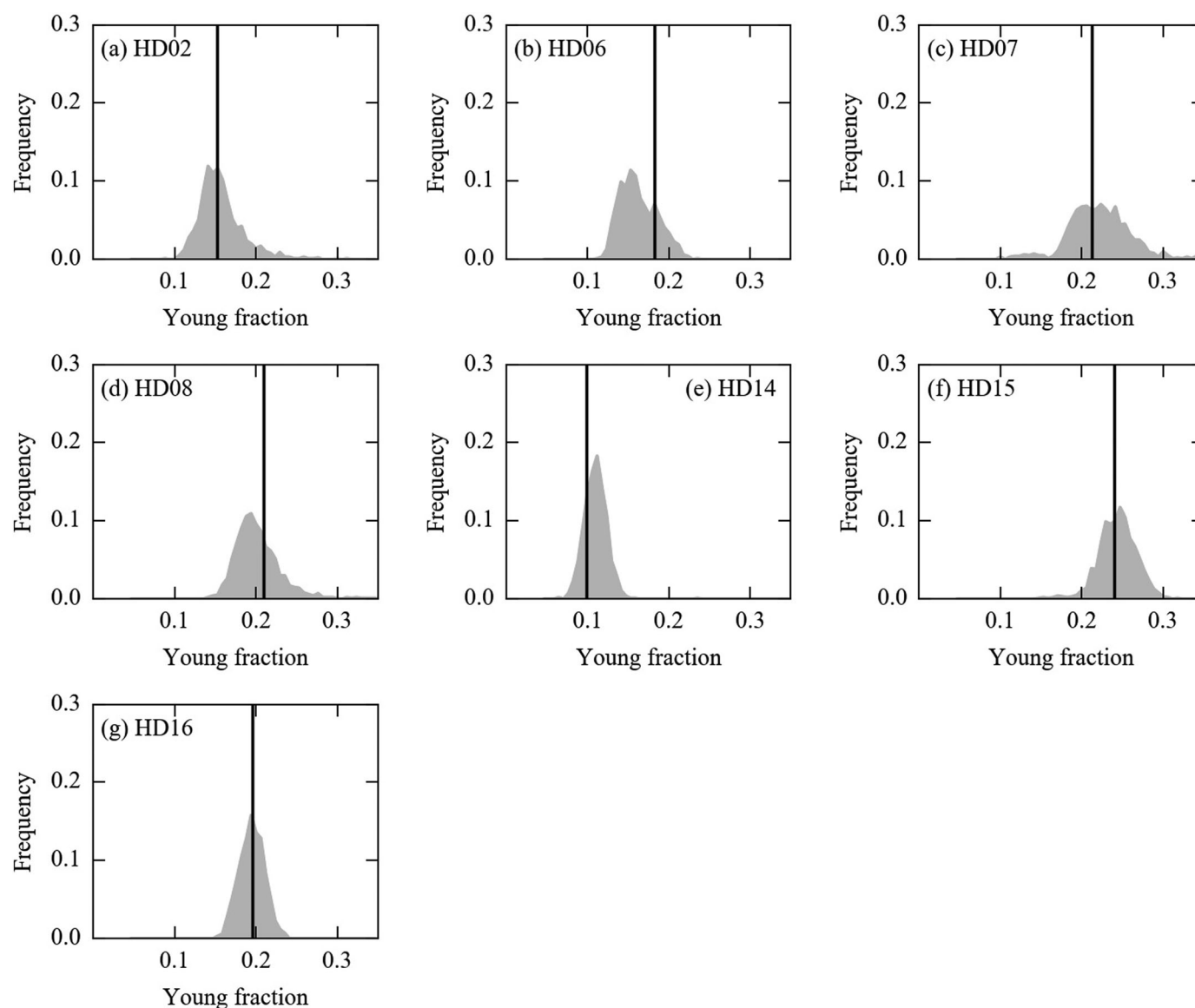


Figure 8. Distribution of estimates of young fraction (water less than 60 years old). The black line represents the best estimate (Table 4). The location of the wells is represented in Figures 1 and 2.

water does not represent the whole distribution, temporal variations in the fraction of young water may give insight into current day management questions.

5. Discussion

In this study, we have used multiple environmental tracers and a shape-free model of age distributions to investigate the impacts of mine dewatering on the natural groundwater flow system. Our results suggest that the multimodal distributions represent a mixture of modern and older groundwater. While the exact age distribution is highly uncertain, the ages of the components that make up the distribution can be identified. These components may be due to variations in recharge with time, long well screens intercepting multiple aquifers or both. Although the proportion of each mode is highly sensitive to errors, the mixture of ages at the sampling location may give significant insight into the time frames of hydrological processes.

We explain the occurrence of multiple modes with the variability in historical recharge patterns. Even wells far from the river had some young water consistent with the occurrence of a recent wet period [Rouillard

et al., 2015]. All wells apart from HD15 contained portions of the water of an age consistent with recharge occurring during the dry period with megafloods (occurring up to 400 years before present). Although the dryer period would suggest less recharge, high rainfall events that generate megafloods, rather than a consistently wetter climate may potentially drive groundwater recharge. The dependence of recharge on high intensity rainfall events is consistent with the findings of *Dogramaci et al.* [2012] that the stable isotope composition of groundwater was consistent in composition with rainfall during high intensity events.

Our study was prone to a number of limitations. Although ideally all our data points would have been collected during a single sampling campaign, ^{39}Ar and ^{85}Kr were collected 1 year after the other tracers. Additionally, the assumption of a piston flow travel time through the unsaturated zone is simplistic. It is also likely that the time lag in the unsaturated zone is a distribution, rather than a single value. We also assumed that gas tracer lags were not important. *Cook and Solomon* [1995] found lag times of 1–2 years for a 30 m unsaturated zone for gas tracers. These lags are an order of magnitude lower than the lags predicted for tritium. We also did not account for retardation [*Massoudieh et al.*, 2012] which could potentially be included in the nonlinear estimation process. The method we used to estimate nonlinear components can also lead to the identification of local rather than global minima. However, the perturbed data demonstrated that a wide range of values could be found for each parameter. Additionally, the method implemented depended on the collection of a relatively large number of tracer data. This may be inhibitive in practice due to the cost of sample analyses.

The method we have implemented here essentially determines the best nonnegative estimate of the age distribution subject to smoothness. Previous studies have used a finite number of distinct ages [*Jurgens et al.*, 2014] or age bins [*Massoudieh et al.*, 2014; *Visser et al.*, 2013] to interpret environmental tracer data. While using a large number of bins allows for the detailed age distributions, the limited amount of data likely results in an over-smoothing of the age distribution. While this limits the identification of exact periods, it does make the appearance of two modes more significant, as ideally the preference would be for a smooth solution. Although the method is not likely to be an exact estimate of the age distributions, the ability to identify the existence of older and younger water without a predefined model is a reasonable result based on our knowledge of the system.

When presenting the entire distribution as a mean age, a significant amount of information about the age distribution may be lost especially when the ages are multimodal. In some cases, the mean age may represent the predominant mode. This appears to be the case for wells HD07 and HD08. In other cases, the mean age lies somewhere between the major modes which reduces the usefulness of the metric and is also the case for well HD02 and HD15. This inability to represent combined distributions has also been noted as aggregation error [*Kirchner*, 2016; *Stewart et al.*, 2016]. Additionally, the tracers used may truncate the range of ages used to represent the mean. Here we truncated our age distributions at 20,000 years as this represented the range over which Carbon-14 was present in samples. The drawback of this approach was observed in estimates from well HD16, where a large amount of water was required in the oldest age bin. This suggests the presence of even older water which cannot be quantified and dated with the tracers used in our study. An alternative indicator could be the median age, which represents the age where the cumulative distribution is 0.5, making it less sensitive to the errors in fractions of old water where limited tracer data are available.

The work presented here goes beyond previous studies in that it overcomes the limitations of single tracer approaches and the use of assumed models of groundwater age distributions. In doing this we were able to separate distinct age ranges that correspond to recharge time frames. Identifying distinct age ranges allowed for the determination of recharge variability on the scale of climate variability at our site giving important insight into the groundwater replenishment mechanisms.

Further work should involve continued monitoring of the wells at the site which would allow us to further identify the transition of the system for the prepumping condition to a new condition. The timeframes of this change may also be of interest in determining the time taken to reach prepumping conditions. It is also of interest to identify the mechanisms—e.g., paleoclimate, sampling conditions, and well placement that lead to the distributions observed here.

6. Conclusions

In this study, we presented a multitracer technique with shape-free analysis to assess the impacts of mine dewatering on groundwater flow in the Pilbara region of north-west Australia. The technique we used has

allowed us to identify the occurrence of distinct age components. Our results suggest that most of the groundwater at the site is made up of four distinct components—local diffuse recharge with ages between zero and 20 years, recharge from Weeli Wolli Creek with ages between 50 and 200 years and two regional components with ages of 100–600 years and 1000–2000 years. The regional components may be representative of paleoclimatic conditions or due to long screens intersecting multiple aquifers.

Appendix A: Details of Deconvolution Procedure

In addition to the relationship between tracer concentration and groundwater ages presented in equation (4), a number of other constraints need to be added. First, age distributions need to adhere to a strict nonnegativity [Cirpka *et al.*, 2007]. Additionally, when applied to age, especially when using tracers present in waters over a large range of ages (i.e., Carbon-14), the distribution needs to integrate to unity. The procedure presented to preserve nonnegativity has been applied to a number of applications [Fienen *et al.*, 2006; Cirpka *et al.*, 2007; Luo and Cirpka, 2008; Payn *et al.*, 2008; Liao *et al.*, 2014; McCallum *et al.*, 2014b]. This results in a general procedure to add and remove constraints for non-negativity iteratively until the ages the constraints are applied to do not change between iterations.

The constraint for unity has been applied previously for problems either as a definite constraint [McCallum *et al.*, 2014b] or added and removed depending on if the integral exceeds one [Liao *et al.*, 2014]. As we are using Carbon-14 which contains some recharge concentration at all times measured, the constraint for unity was added at all times which was achieved by using the relationship:

$$\mathbf{d}\boldsymbol{\tau}^T\mathbf{g}=1 \quad (\text{A1})$$

where $\mathbf{d}\boldsymbol{\tau}$ is a vector of discrete values of the age step.

Finally, as the age distributions we estimated were more detailed than the number of observations allowed, we added a constraint of smoothness. Here we used a variogram approach similar to Cirpka *et al.* [2007]. Here we define the expected difference between two discrete values as a linear function of the difference in the ages they represent:

$$E\left[\frac{1}{2}(g(\tau+h)-g(\tau))\right]=\theta|h| \quad (\text{A2})$$

where h is a lag distance and θ is the slope of the linear variogram. The smoothness can be represented as a matrix (Γ_{gg}) of discrete semivariogram values where $\Gamma_{ij}=\theta|\tau_i-\tau_j|$. Accounting for errors and constraints, the final equation can be presented as:

$$\begin{bmatrix} \mathbf{X}^T\mathbf{Q}\mathbf{X}+\Gamma_{gg}^{-1} & \mathbf{H}^T & \mathbf{d}\boldsymbol{\tau}^T \\ \mathbf{H} & 0 & 0 \\ \mathbf{d}\boldsymbol{\tau} & 0 & 0 \end{bmatrix} \begin{bmatrix} \mathbf{g} \\ \mathbf{v} \\ \mathbf{v}_1 \end{bmatrix} = \begin{bmatrix} \mathbf{X}^T\mathbf{Q}\mathbf{c}_g \\ \mathbf{0} \\ \mathbf{1} \end{bmatrix} \quad (\text{A3})$$

where \mathbf{Q} is a diagonal matrix containing values of $\frac{1}{\sigma^2}$ where σ is the error of the concentrations, \mathbf{H} is the matrix of constraints for nonnegativity [see McCallum *et al.*, 2014a,b], and \mathbf{v} and \mathbf{v}_1 are the Lagrange multipliers that represent the constraints of nonnegativity and unity. The equations are solved iteratively by adding and removing nonnegativity constraints until the location of the constraints no longer changes.

A1. Estimation of Variogram Parameter

In the case we have presented, we have assumed and specified the elements of the matrix \mathbf{Q} . The slope of the variogram can be estimated. Here we define another matrix \mathbf{R} , where $\mathbf{R}_{ij}=|\tau_i-\tau_j|$. The slope parameter θ can then be estimated using a chi squared test by minimizing [Mead, 2008]:

$$\mathbf{c}_g^T(\mathbf{X}[\theta\mathbf{R}]^{-1})\mathbf{X}^T-\mathbf{Q})\mathbf{c}_g-nc=0 \quad (\text{A4})$$

All calculations were carried out using the NumPy [van der Walt *et al.*, 2011] extension of Python. Equation A4 was solved using the fsolve function, a minimization function available in the SciPy package for Python [Jones *et al.*, 2001; Oliphant, 2007].

Acknowledgments

This research was undertaken as part of a collaborative project between Rio Tinto Iron Ore (RTIO) and the National Centre for Groundwater Research and Training. Funding was provided by RTIO and the Australian Research Council through Linkage grant LP150100395. The authors wish to thank Jodi Mead for assistance with regularization weighting. Measurement and analysis of atmospheric Krypton-85 was undertaken by Bundesamt für Strahlenschutz and raw data were provided by Clemens Schlosser. We thank Olaf Cirpka, Werner Aeschbach, and two anonymous reviewers for their constructive feedback. The models used for data analysis can be obtained by contacting the lead author.

References

- Althaus, R., S. Klump, A. Onnis, R. Kipfer, R. Purtschert, F. Stauffer, and W. Kinzelbach (2009), Noble gas tracers for characterisation of flow dynamics and origin of groundwater: A case study in Switzerland, *J. Hydrol.*, *370*(1–4), 64–72, doi:10.1016/j.jhydrol.2009.02.053.
- Becker, R. H., and R. N. Clayton (1972), Carbon isotopic evidence for the origin of a banded iron-formation in Western Australia, *Geochim. Cosmochim. Acta*, *36*(5), 577–595, doi:10.1016/0016-7037(72)90077-4.
- Bentley, H. W., F. M. Phillips, S. N. Davis, M. A. Habermehl, P. L. Airey, G. E. Calf, D. Elmore, H. E. Gove, and T. Torgersen (1986), Chlorine 36 dating of very old groundwater: 1. The Great Artesian Basin, Australia, *Water Resour. Res.*, *22*(13), 1991–2001, doi:10.1029/WR022i013.p01991.
- Bethke, C. M., and T. M. Johnson (2002), Paradox of groundwater age: Correction 1, *Geology*, *30*(4), 385, doi:10.1130/0091-7613(2002)030<0386:POGAC>2.0.CO;2.
- Bollhöfer, a., C. Schlosser, J. O. Ross, H. Sartorius, and S. Schmid (2014), Variability of atmospheric krypton-85 activity concentrations observed close to the ITCZ in the southern hemisphere, *J. Environ. Radioact.*, *127*, 111–118, doi:10.1016/j.jenvrad.2013.10.003.
- Brinkman, R., K. O. Münnich, and J. C. Vogel (1959), 14C Altersbestimmungen von Grundwasser, *Naturwissenschaften*, *46*, 10–12.
- Bullister, J. L. (2015), *Atmospheric Histories (1765–2015) for CFC-11, CFC-12, CFC-113, CCl4, SF6 and N2O*, Carbon Dioxide Information Analysis Center, Oak Ridge National Laboratory, US Department of Energy, Oak Ridge, Tennessee, doi: 10.3334/CDIAC/otg.CFC_ATM_Hist_2015.
- Busenberg, E., and L. N. Plummer (2000), Dating young groundwater with sulfur hexafluoride: Natural and anthropogenic sources of sulfur hexafluoride, *Water Resour. Res.*, *36*(10), 3011–3030, doi:10.1029/2000WR900151.
- Busenberg, E., and L. N. Plummer (2008), Dating groundwater with trifluoromethyl sulfurpentafluoride (SF₅SCF₃), sulfur hexafluoride (SF₆), CF₃Cl (CFC-13), and CF₂Cl₂ (CFC-12), *Water Resour. Res.*, *44*, W02431, doi:10.1029/2007WR006150.
- Cardenas, M. B. (2008), Surface water-groundwater interface geomorphology leads to scaling of residence times, *Geophys. Res. Lett.*, *35*, L08402, doi:10.1029/2008GL033753.
- Cirpka, O. a., M. N. Fienen, M. Hofer, E. Hoehn, A. Tessarini, R. Kipfer, and P. K. Kitanidis (2007), Analyzing bank filtration by deconvoluting time series of electric conductivity, *Ground Water*, *45*(3), 318–328, doi:10.1111/j.1745-6584.2006.00293.x.
- Cook, P. G., and D. K. Solomon (1995), Transport of atmospheric trace gases to the water table: Implications for groundwater dating with chlorofluorocarbons and Krypton 85, *Water Resour. Res.*, *31*(2), 263–270, doi:10.1029/94WR02232.
- Cook, P. G., D. K. Solomon, L. N. Plummer, E. Busenberg, and S. L. Schiff (1995), Chlorofluorocarbons as tracers of groundwater transport processes in a shallow, silty sand aquifer, *Water Resour. Res.*, *31*(3), 425–434, doi:10.1029/94WR02528.
- Cook, P. G., S. Dogramaci, J. L. McCallum, and J. Hedley (2016), Groundwater age, mixing and flow rates in the vicinity of large open pit mines, Pilbara region northwestern Australia, *Hydrogeol. J.*, doi:10.1007/s10040-016-1467-y, in press.
- Corcho Alvarado, J. A., R. Purtschert, F. Barbécot, C. Chabault, J. Rueedi, V. Schneider, W. Aeschbach-Hertig, R. Kipfer, and H. H. Loosli (2007), Constraining the age distribution of highly mixed groundwater using 39Ar: A multiple environmental tracer (3H/3He, 85Kr, 39Ar, and 14C) study in the semiconfined Fontainebleau Sands Aquifer (France), *Water Resour. Res.*, *43*, W03427, doi:10.1029/2006WR005096.
- Corcho Alvarado, J. A., T. Pačes, and R. Purtschert (2013), Dating groundwater in the Bohemian Cretaceous Basin: Understanding tracer variations in the subsurface, *Appl. Geochem.*, *29*, 189–198, doi:10.1016/j.apgeochem.2012.11.014.
- Cornaton, F. J., Y.-J. Park, and E. Deleersnijder (2011), On the biases affecting water ages inferred from isotopic data, *J. Hydrol.*, *410*(3–4), 217–225, doi:10.1016/j.jhydrol.2011.09.024.
- Dogramaci, S., G. Skrzypek, W. Dodson, and P. F. Grierson (2012), Stable isotope and hydrochemical evolution of groundwater in the semi-arid Hamersley Basin of subtropical northwest Australia, *J. Hydrol.*, *475*, 281–293, doi:10.1016/j.jhydrol.2012.10.004.
- Dörr, H., U. Werner, S. Drenkhard, R. Bayer, and P. Schlosser (1995), The use of isotope methods in groundwater protection studies, *Isot. Environ. Health Stud.*, *31*(1), 47–59, doi:10.1080/10256019508036252.
- Edmunds, W. M., W. G. Darling, R. Purtschert, and J. A. Corcho Alvarado (2014), Noble gas, CFC and other geochemical evidence for the age and origin of the Bath thermal waters, UK, *Appl. Geochem.*, *40*, 155–163, doi:10.1016/j.apgeochem.2013.10.007.
- Ekwurzel, B., P. Schlosser, W. M. Smethie, L. N. Plummer, E. Busenberg, R. L. Michel, R. Weppernig, and M. Stute (1994), Dating of shallow groundwater: Comparison of the transient tracers 3H/3He, chlorofluorocarbons and 85Kr, *Water Resour. Res.*, *30*(6), 1693–1708, doi:10.1029/94WR00156.
- Engdahl, N. B., T. R. Ginn, and G. E. Fogg (2012), Non-Fickian dispersion of groundwater age, *Water Resour. Res.*, *48*, W07508, doi:10.1029/2012WR012251.
- Engdahl, N. B., J. L. McCallum, and A. Massoudieh (2016), Transient age distributions in subsurface hydrologic systems, *J. Hydrol.*, *543*, 88–100, doi:10.1016/j.jhydrol.2016.04.066.
- Etcheverry, D., and P. Perrochet (2000), Direct simulation of groundwater transit-time distributions using the reservoir theory, *Hydrogeol. J.*, *8*(2), 200–208, doi:10.1007/s100400050006.
- Fienen, M. N., J. Luo, and P. K. Kitanidis (2006), A Bayesian geostatistical transfer function approach to tracer test analysis, *Water Resour. Res.*, *42*, W07426, doi:10.1029/2005WR004576.
- Gleeson, T., K. M. Befus, S. Jasechko, E. Luijendijk, and M. B. Cardenas (2016), The global volume and distribution of modern groundwater, *Nat. Geosci.*, *9*(2), 161–167, doi:10.1038/ngeo2590.
- Goode, D. J. (1996), Direct simulation of groundwater age, *Water Resour. Res.*, *32*(2), 289–296, doi:10.1029/95WR03401.
- Green, C. T., J. K. Bohlke, B. A. Bekins, and S. P. Phillips (2010), Mixing effects on apparent reaction rates and isotope fractionation during denitrification in a heterogeneous aquifer, *Water Resour. Res.*, *46*, W08525, doi:10.1029/2009WR008903.
- Han, L. F., and L. N. Plummer (2013), Revision of Fontes & Garnier's model for the initial 14C content of dissolved inorganic carbon used in groundwater dating, *Chem. Geol.*, *351*, 105–114, doi:10.1016/j.chemgeo.2013.05.011.
- Hinsby, K., A. L. Højberg, P. Engesgaard, K. H. Jensen, F. Larsen, L. N. Plummer, and E. Busenberg (2007), Transport and degradation of chlorofluorocarbons (CFCs) in the pyritic Rabis Creek aquifer, Denmark, *Water Resour. Res.*, *43*, W10423, doi:10.1029/2006WR005854.
- Hofmann, T., A. Darsow, M. Gröning, P. Aggarwal, and A. Suckow (2010), Direct-push profiling of isotopic and hydrochemical vertical gradients, *J. Hydrol.*, *385*(1–4), 84–94, doi:10.1016/j.jhydrol.2010.02.005.
- International Atomic Energy Agency / World Meteorological Organization (2016), *Global Network of Isotopes in Precipitation, The GNIP Database*. [Available at <http://www.iaea.org/water/>]
- Jasechko, S. (2016), Partitioning young and old groundwater with geochemical tracers, *Chem. Geol.*, *427*, 35–42, doi:10.1016/j.chemgeo.2016.02.012.
- Jasechko, S., S. J. Birks, T. Gleeson, Y. Wada, P. J. Fawcett, Z. D. Sharp, J. J. McDonnell, and J. M. Welker (2014), The pronounced seasonality of global groundwater recharge, *Water Resour. Res.*, *50*, 8845–8867, doi:10.1002/2014WR015809.

- Jasechko, S. et al. (2015), Intensive rainfall recharges tropical groundwaters, *Environ. Res. Lett.*, 10(12), 124015, doi:10.1088/1748-9326/10/12/124015.
- Jones, E., et al. (2001), *SciPy: Open Source Scientific Tools for Python*. [Available at <http://www.scipy.org/>, accessed 24 Nov, 2016.]
- Jurgens, B. C., L. M. Bexfield, and S. M. Eberts (2014), A Ternary age-mixing model to explain contaminant occurrence in a deep supply well, *Groundwater*, 52, 25–39, doi:10.1111/gwat.12170.
- Kirchner, J. W. (2016), Aggregation in environmental systems - Part 1: Seasonal tracer cycles quantify young water fractions, but not mean transit times, in spatially heterogeneous catchments, *Hydrol. Earth Syst. Sci.*, 20(1), 279–297, doi:10.5194/hess-20-279-2016.
- Lehmann, B. E., S. N. Davis, and J. T. Fabryka-Martin (1993), Atmospheric and subsurface sources of stable and radioactive nuclides used for groundwater dating, *Water Resour. Res.*, 29(7), 2027–2040, doi:10.1029/93WR00543.
- Leray, S., J. R. de Dreuz, L. Aquilina, V. Vergnaud-Ayraud, T. Labasque, O. Bour, and T. Le Borgne (2014), Temporal evolution of age data under transient pumping conditions, *J. Hydrol.*, 511, 555–566, doi:10.1016/j.jhydrol.2014.01.064.
- Leray, S., N. B. Engdahl, A. Massoudieh, E. Bresciani, and J. McCallum (2016), Residence time distributions for hydrologic systems: Mechanistic foundations and steady-state analytical solutions, *J. Hydrol.*, 543, 67–87, doi:10.1016/j.jhydrol.2016.01.068.
- Liao, Z., K. Osenbrück, and O. A. Cirpka (2014), Non-stationary nonparametric inference of river-to-groundwater travel-time distributions, *J. Hydrol.*, 519, 3386–3399, doi:10.1016/j.jhydrol.2014.09.084.
- Loosli, H. H., and R. Purtschert (2005), Rare gases, in *Isotopes in the Water Cycle: Past, Present and Future of a Developing Science*, edited by P. Aggarwal, J. R. Gat, and K. Froehlich, pp. 91–95, IAEA, Vienna.
- Loosli, H. H., M. Möll, H. Oeschger, and U. Schotterer (1986), Ten years low-level counting in the underground laboratory in Bern, Switzerland, *Nucl. Instrum. Methods Phys. Res. Sect. B*, 17(5–6), 402–405, doi:10.1016/0168-583X(86)90172-2.
- Luo, J., and O. A. Cirpka (2008), Traveltime-based descriptions of transport and mixing in heterogeneous domains, *Water Resour. Res.*, 44, W09407, doi:10.1029/2007WR006035.
- Maloszewski, P., and A. Zuber (1982), Determining the turnover time of groundwater systems with the aid of environmental tracers, *J. Hydrol.*, 57(3–4), 207–231, doi:10.1016/0022-1694(82)90147-0.
- Manning, A. H., J. F. Clark, S. H. Diaz, L. K. Rademacher, S. Earman, and L. Niel Plummer (2012), Evolution of groundwater age in a mountain watershed over a period of thirteen years, *J. Hydrol.*, 460–461, 13–28, doi:10.1016/j.jhydrol.2012.06.030.
- Manning, M., D. Lowe, W. H. Melhuish, R. J. Sparks, G. Wallace, C. A. Brenninkmeijer, and R. C. McGill (1990), The use of radiocarbon measurements in atmospheric studies, *Radiocarbon*, 32(1), 37–58.
- Massoudieh, A. (2013), Inference of long-term groundwater flow transience using environmental tracers: A theoretical approach, *Water Resour. Res.*, 49, 8039–8052, doi:10.1002/2013WR014548.
- Massoudieh, A., S. Sharifi, and D. K. Solomon (2012), Bayesian evaluation of groundwater age distribution using radioactive tracers and anthropogenic chemicals, *Water Resour. Res.*, 48, W09529, doi:10.1029/2012WR011815.
- Massoudieh, A., A. Visser, S. Sharifi, and H. P. Broers (2014), A Bayesian modeling approach for estimation of a shape-free groundwater age distribution using multiple tracers, *Appl. Geochem.*, 50, 252–264.
- McCallum, J. L., P. G. Cook, C. T. Simmons, and A. D. Werner (2014a), Bias of Apparent Tracer Ages in Heterogeneous Environments, *Groundwater*, 52(2), 239–250, doi:10.1111/gwat.12052.
- McCallum, J. L., N. B. Engdahl, T. R. Ginn, and P. G. Cook (2014b), Nonparametric estimation of groundwater residence time distributions: What can environmental tracer data tell us about groundwater residence time?, *Water Resour. Res.*, 50, 2022–2038, doi:10.1002/2013WR014974.
- McCallum, J. L., P. G. Cook, and C. T. Simmons (2015), Limitations of the Use of Environmental Tracers to Infer Groundwater Age, *Groundwater*, 53(S1), 56–70, doi:10.1111/gwat.12237.
- McMahon, P. B., L. N. Plummer, J. K. Bohlke, S. D. Shapiro, and S. R. Hinkle (2011), A comparison of recharge rates in aquifers of the United States based on groundwater-age data, *Hydrogeol. J.*, 19(4), 779–800, doi:10.1007/s10040-011-0722-5.
- Mead, J. L. (2008), A priori weighting for parameter estimation, *J. Inverse Ill-Pos. Probl.*, 16(2), 175–193, doi:10.1515/JIIP.2008.011.
- Morgenstern, U., and C. B. Taylor (2009), Ultra low-level tritium measurement using electrolytic enrichment and LSC, *Isotopes Environ. Health Stud.*, 45(2), 96–117, doi:10.1080/10256010902931194.
- Nelder, J. A., and R. Mead (1965), A simplex method for function minimization, *Comput. J.*, 7(4), 308–313, doi:10.1093/comjnl/7.4.308.
- Nir, A. (1964), On the interpretation of tritium “age” measurements of groundwater, *J. Geophys. Res.*, 69(12), 2589–2595, doi:10.1029/JZ069i012p02589.
- Oliphant, T. E. (2007), Python for scientific computing, *Comput. Sci. Eng.*, 9(3), 10–20, doi:10.1109/MCSE.2007.58.
- Park, J., C. M. Bethke, T. Torgersen, and T. M. Johnson (2002), Transport modeling applied to the interpretation of groundwater Cl-36 age, *Water Resour. Res.*, 38(5), 1043, doi:10.1029/2001WR000399.
- Payn, R. A., M. N. Gooseff, D. A. Benson, O. A. Cirpka, J. P. Zarnetske, W. B. Bowden, J. P. McNamara, and J. H. Bradford (2008), Comparison of instantaneous and constant-rate stream tracer experiments through non-parametric analysis of residence time distributions, *Water Resour. Res.*, 44, W06404, doi:10.1029/2007WR006274.
- Purtschert, R., N. C. Sturchio, and R. Yokochi (2013), Krypton-81 dating of old groundwater, in *Isotope Methods for Dating Old Groundwater*, edited by A. Suckow, P. Aggarwal, and L. Araguas-Araguas, pp. 91–124, IAEA, Vienna.
- Riedmann, R. A., and R. Purtschert (2016), Separation of argon from environmental samples for Ar-37 and Ar-39 analyses, *Sep. Purif. Technol.*, 170, 217–223, doi:10.1016/j.seppur.2016.06.017.
- Ross, J. O. (2010), Simulation of atmospheric krypton-85 transport to assess the detectability of clandestine nuclear reprocessing, Reports on earth systems science 82/2010, Max Planck Institute for Meteorology, Hamburg.
- Rouillard, A., G. Skrzypek, S. Dogramaci, C. Turney, and P. F. Grierson (2015), Impacts of high inter-annual variability of rainfall on a century of extreme hydrologic regime of northwest Australia, *Hydrol. Earth Syst. Sci.*, 19(4), 2057–2078, doi:10.5194/hess-19-2057-2015.
- Rouillard, A., G. Skrzypek, C. Turney, S. Dogramaci, Q. Hua, A. Zawadzki, J. Reeves, P. Greenwood, A. J. O'Donnell, and P. F. Grierson (2016), Evidence for extreme floods in arid subtropical northwest Australia during the Little Ice Age chronozone (CE 1400–1850), *Quat. Sci. Rev.*, 144, 107–122, doi:10.1016/j.quascirev.2016.05.004.
- Sanford, W. E. (1997), Correcting for Diffusion in Carbon-14 Dating of Ground Water, *Ground Water*, 35(2), 357–361, doi:10.1111/j.1745-6584.1997.tb00093.x.
- Sardin, M., D. Schweich, F. J. Leij, and M. T. van Genuchten (1991), Modeling the Nonequilibrium Transport of Linearly Interacting Solutes in Porous Media: A Review, *Water Resour. Res.*, 27(9), 2287–2307, doi:10.1029/91WR01034.
- Schwartz, F. W., E. A. Sudicky, R. G. McLaren, Y.-J. Park, M. Huber, and M. Apte (2010), Ambiguous hydraulic heads and 14C activities in transient regional flow, *Ground Water*, 48(3), 366–79, doi:10.1111/j.1745-6584.2009.00655.x.

- Schwientek, M., P. Maloszewski, and F. Einsiedl (2009), Effect of the unsaturated zone thickness on the distribution of water mean transit times in a porous aquifer, *J. Hydrol.*, 373(3-4), 516–526, doi:10.1016/j.jhydrol.2009.05.015.
- Solomon, D. K., D. P. Genereux, L. N. Plummer, and E. Busenberg (2010), Testing mixing models of old and young groundwater in a tropical lowland rain forest with environmental tracers, *Water Resour. Res.*, 46, W04518, doi:10.1029/2009WR008341.
- Stewart, M. K., U. Morgenstern, M. A. Gusyev, and P. Maloszewski (2016), Aggregation effects on tritium-based mean transit times and young water fractions in spatially heterogeneous catchments and groundwater systems, and implications for past and future applications of tritium, *Hydrol. Earth Syst. Sci. Discuss.*, 1–26, doi:10.5194/hess-2016-532.
- Stolp, B. J., D. K. Solomon, a. Suckow, T. Vitvar, D. Rank, P. K. Aggarwal, and L. F. Han (2010), Age dating base flow at springs and gaining streams using helium-3 and tritium: Fischa-Dagnitz system, southern Vienna Basin, Austria, *Water Resour. Res.*, 46, W07503, doi:10.1029/2009WR008006.
- Sudicky, E. A., and E. O. Frind (1981), Carbon 14 dating of groundwater in confined aquifers: Implications of aquitard diffusion, *Water Resour. Res.*, 17(4), 1060–1064, doi:10.1029/WR017i004p01060.
- Tadros, C. V., C. E. Hughes, J. Crawford, S. E. Hollins, and R. Chisari (2014), Tritium in Australian precipitation: A 50 year record, *J. Hydrol.*, 513, 262–273, doi:10.1016/j.jhydrol.2014.03.031.
- Taylor, R. G., M. C. Todd, L. Kongola, L. Maurice, E. Nahozya, H. Sanga, and A. M. MacDonald (2012a), Evidence of the dependence of groundwater resources on extreme rainfall in East Africa, *Nat. Clim. Change*, 3(4), 374–378, doi:10.1038/nclimate1731.
- Taylor, R. G. et al. (2012b), Ground water and climate change, *Nat. Clim. Change*, 3(4), 322–329, doi:10.1038/nclimate1744.
- van der Walt, S., S. C. Colbert, and G. Varoquaux (2011), The NumPy array: A structure for efficient numerical computation, *Comput. Sci. Eng.*, 13(2), 22–30, doi:10.1109/MCSE.2011.37.
- Varni, M., and J. Carrera (1998), Simulation of groundwater age distributions, *Water Resour. Res.*, 34(12), 3271–3281.
- Visser, A., J. D. Schaap, H. P. Broers, and M. F. P. Bierkens (2009), Degassing of 3H/3He, CFCs and SF6 by denitrification: Measurements and two-phase transport simulations, *J. Contam. Hydrol.*, 103(3-4), 206–218, doi:10.1016/j.jconhyd.2008.10.013.
- Visser, A., H. P. Broers, R. Purtschert, J. Sültenfuß, and M. De Jonge (2013), Groundwater age distributions at a public drinking water supply well field derived from multiple age tracers (85Kr, 3H/3He, and 39Ar), *Water Resour. Res.*, 49, 7778–7796, doi:10.1002/2013WR014012.
- Vogel, J. C., L. Thilo, and M. Van Dijken (1974), Determination of groundwater recharge with tritium, *J. Hydrol.*, 23(1), 131–140, doi:10.1016/0022-1694(74)90027-4.
- Waugh, D. W., T. M. Hall, and T. W. N. Haine (2003), Relationships among tracer ages, *J. Geophys. Res.*, 108(C5), 3138, doi:10.1029/2002JC001325.
- Weiss, W., H. Sartorius, and H. Stockburger (1992), Global distribution of atmospheric ⁸⁵Kr. A database for the verification of transport and mixing models, in *Isotopes of Noble Gases as Tracers in Environmental Studies*, edited by H. H. Loosli and E. Mazor, Atomic Energy Agency (IAEA), Vienna, Austria.
- Weissmann, G. S., Y. Zhang, E. M. Labolle, and G. E. Fogg (2002), Dispersion of groundwater age in an alluvial aquifer system, *Water Resour. Res.*, 38(10), 1198, doi:10.1029/2001WR000907.
- Winger, K., J. Feichter, M. B. Kalinowski, H. Sartorius, and C. Schlosser (2005), A new compilation of the atmospheric 85krypton inventories from 1945 to 2000 and its evaluation in a global transport model, *J. Environ. Radioact.*, 80(2), 183–215, doi:10.1016/j.jenvrad.2004.09.005.